NeuroImage: Clinical 38 (2023) 103410

Contents lists available at ScienceDirect

NeuroImage: Clinical

journal homepage: www.elsevier.com/locate/ynicl

Cognitive and functional connectivity impairment in post-COVID-19 olfactory dysfunction

Lorenzo Muccioli [a,1], Giovanni Sighinolfi [a,1], Micaela Mitolo [b,c], Lorenzo Ferri [a], Magali Jane Rochat [c], Umberto Pensato [d], Lisa Taruffi [a], Claudia Testa [c,e], Marco Masullo [a], Pietro Cortelli [a,c], Raffaele Lodi [a,c], Rocco Liguori [a,c], Caterina Tonon [a,c,2], Francesca Bisulli [a,c,2,*]

[a] Department of Biomedical and Neuromotor Sciences, University of Bologna, Bologna, Italy
[b] Department of Experimental, Diagnostic and Specialty Medicine, University of Bologna, Bologna, Italy
[c] IRCCS Istituto delle Scienze Neurologiche di Bologna, Bologna, Italy
[d] Department of Neurology, IRCCS Humanitas Research Hospital, Milan, Italy
[e] Department of Physics and Astronomy, University of Bologna, Bologna, Italy

ARTICLE INFO

Keywords:
Hyposmia
Long Covid
functional MRI (fMRI)
post acute COVID syndrome (PACS)

ABSTRACT

Objectives: To explore the neuropsychological profile and the integrity of the olfactory network in patients with COVID-19-related persistent olfactory dysfunction (OD).
Methods: Patients with persistent COVID-19-related OD underwent olfactory assessment with Sniffin' Sticks and neuropsychological evaluation. Additionally, both patients and a control group underwent brain MRI, including T1-weighted and resting-state functional MRI (rs-fMRI) sequences on a 3 T scanner. Morphometrical properties were evaluated in olfaction-associated regions; the rs-fMRI data were analysed using graph theory at the whole-brain level and within a standard parcellation of the olfactory functional network. All the MR-derived quantities were compared between the two groups and their correlation with clinical scores in patients were explored.
Results: We included 23 patients (mean age 37 ± 14 years, 12 females) with persistent (mean duration 11 ± 5 months, range 2–19 months) COVID-19-related OD (mean score 23.63 ± 5.32/48, hyposmia cut-off: 30.75) and 26 sex- and age-matched healthy controls. Applying population-derived cut-off values, the two cognitive domains mainly impaired were visuospatial memory and executive functions (17 % and 13 % of patients). Brain MRI did not show gross morphological abnormalities. The lateral orbital cortex, hippocampus, and amygdala volumes exhibited a reduction trend in patients, not significant after the correction for multiple comparisons. The olfactory bulb volumes did not differ between patients and controls. Graph analysis of the functional olfactory network showed altered global and local properties in the patients' group (n = 19, 4 excluded due to artifacts) compared to controls. Specifically, we detected a reduction in the global modularity coefficient, positively correlated with hyposmia severity, and an increase of the degree and strength of the right thalamus functional connections, negatively correlated with short-term verbal memory scores.
Discussion: Patients with persistent COVID-19-related OD showed an altered olfactory network connectivity correlated with hyposmia severity and neuropsychological performance. No significant morphological alterations were found in patients compared with controls.

1. Introduction

Olfactory dysfunction (OD) is a common manifestation of SARS-CoV-2 infection, affecting approximately 50 to 75 % of people diagnosed with COVID-19 (Xydakis et al., 2021). In most cases, recovery of olfactory function is rapid, occurring after a median of 10 days. However, in approximately-one-tenth of the patients, OD may persist for several months (Xydakis et al., 2021; Logue et al., 2021). Cognitive impairment is another frequent manifestation of long-COVID (Graham et al., 2021), a syndrome with variable definitions: either the persistence of COVID-

* Corresponding author at: IRCCS Istituto delle Scienze Neurologiche di Bologna, Bellaria Hospital, Via Altura 3, Bologna 40139, Italy.
E-mail address: francesca.bisulli@unibo.it (F. Bisulli).
[1] These authors contributed equally to this work.
[2] These authors contributed equally to this work.

https://doi.org/10.1016/j.nicl.2023.103410
Received 24 October 2022; Received in revised form 13 April 2023; Accepted 15 April 2023
Available online 17 April 2023

19-related symptoms for ≥ 4 weeks after initial infection (Nalbandian et al., 2021) or the persistence of symptoms at three months post-infection, with a duration of at least two months, without other explanatory causes (Post COVID-19 condition (Long COVID), Accessed March 8, 2023). Previous studies have associated COVID-19-related OD with cognitive dysfunction, yet with either limited neuropsychological testing or olfactory assessment (Esposito et al., 2022; Pirker-Kees et al., 2021; Cristillo et al., 2021; Llana et al., 2022; Voruz et al., 2022).

The pathophysiology underlying COVID-19-related OD is still debated. It may involve disrupting the olfactory system at different levels, from the sensory epithelium located in the olfactory clefts to olfactory neurons in the olfactory bulb and olfactory cortices (Xydakis et al., 2021). Previous magnetic resonance imaging (MRI) studies revealed a variety of abnormalities of both peripheral and central olfactory areas, including olfactory cleft obstruction, abnormalities in olfactory bulb signal intensity and atrophy, and, notably, neurodegenerative changes in the limbic structures involved in the processing of olfactory stimuli and cognitive functions, also in patients with persistent OD (Kandemirli et al., 2021; Keshavarz et al., 2021; Yildirim et al., 2022; Douaud et al., 2022; Capelli et al., 2023). Task-based olfactory functional MRI (fMRI) in COVID-19-related OD revealed absent activation of the orbitofrontal cortex and a more robust activation in the trigeminosensory activity (Yildirim et al., 2022; Ismail and Gad, 2021). Resting-state fMRI (rs-fMRI) represents an innovative, alternative technique to study the functional connectivity (FC) of the olfactory network, which may provide additional elements to task-based fMRI, as regions involved in olfactory tasks are not necessarily chemosensory in nature or activated by active sniffing (Lu et al., 2019; Tobia et al., 2016). A higher internetwork connectivity between olfactory and default mode networks has been described in patients with post-COVID hyposmia (Zhang et al., 2022). Regarding neuropsychological features, rs-fMRI graph theory-based analysis has an emerging role in topological explorations of the complex brain connections, with a dramatically increasing number of studies reported since the launch of the Human Connectome Project in 2009 (Farahani et al., 2019). Graph analysis applied to rs-fMRI can quantitatively characterize the connectivity pattern among brain elements (Farahani et al., 2019).

A previous study reported graph-based network analysis of rs-fMRI in patients with COVID-19-related OD during the early stage of recovery (≤3 weeks), showing abnormalities in the FC of the anterior piriform cortex (Esposito et al., 2022). Yet, the connectivity properties of the olfactory network in patients with long-lasting OD and its association with neuropsychological findings remain to be explored. Considering the high prevalence of long-COVID and the mounting evidence suggesting neurodegeneration in COVID-19 survivors (Douaud et al., 2022), it is paramount to characterize this condition better and elucidate the underlying mechanisms.

Herein, we aimed to explore the integrity of the olfactory network in a cohort of patients with COVID-19-related persistent OD through brain morphometry and graph-based network analysis of rs-fMRI and assess its association with the neuropsychological profile.

2. Methods

2.1. Study population and protocol

We prospectively recruited consecutive patients referred to our institute (IRCCS Istituto delle Scienze Neurologiche di Bologna, Bologna, Italy) from February 2021 to November 2021 for persistent (≥1 month) OD with onset during COVID-19 infection, confirmed by an antigen or molecular-based test for SARS-CoV-2. Of note, from June 2021 the Delta variant became dominant in Italy (https://www.epicentro.iss.it/coronavirus/pdf/sars-cov-2-monitoraggio-varianti-rapporti-periodici-26-novembre-2021.pdf). Patients with preexisting OD, chronic rhinosinusitis, and cognitive impairment were excluded. Each participant underwent clinical interview, olfactory assessment, and brain MRI scan in a day. Neuropsychological assessment was performed within one week in all patients.

We also selected a control group of healthy subjects, matched for sex and age with the patient group, from the database of the Neuroimaging Lab at our institute. Healthy controls underwent the same MRI protocol as the OD cohort, but they were not administered the olfactory and neuropsychological evaluations. However, they did not report previous COVID-19 infection or any olfactory, cognitive or neurological deficit at the time of the MRI exam or previously.

2.2. Olfactory function assessment

Patients were thoroughly interviewed on symptoms of OD, either quantitative (hyposmia and anosmia) or qualitative (dysosmia, which includes *parosmia*, defined as distortion of perceived odor quality-, *cacosmia*, or unpleasant distortion of perceived odor quality, and *phantosmia*, or olfactory hallucinations), and associated subjective gustatory dysfunction. Subsequently, olfactory performance was evaluated objectively with the widely used "Sniffin' Sticks" test (Burghart Messtechnik, Wedel, Germany) (Kobal et al., 1996). This consists of three subtests: olfactory threshold (T), odor discrimination (D), and odor identification (I), each with a score ranging from 1 to 16. TDI is the summative score of the three components, ranging from 3 to 48. Olfactory function is categorized as functional anosmia (TDI score ≤ 16.00), hyposmia (TDI score between 16.25 and 30.50), or normosmia (TDI score ≥ 30.75, with "supersmellers" scoring ≥ 41.50 points) (Oleszkiewicz et al., 2019). Gustatory function was not assessed by a dedicated test but only reported during the interview.

2.3. Neuropsychological evaluation

Years of education and handedness dominance using the Edinburgh Handedness Inventory (EHI) (Oldfield, 1971) were calculated for all patients and controls.

All patients were administered a standardized battery, composed by eleven neuropsychological tests (Barletta-Rodolfi et al., 2011; Lovibond and Lovibond, 1995; Larson, 2013; Evangelisti et al., 2019; Evangelisti et al., 2018), including a general screening test (i.e., Montreal Cognitive Assessment MoCA). Language skills were assessed using an Associative Fluency Test and a Category Words Fluency Test.

Verbal and visuospatial short-term memory span were assessed using the Digit Span forward test and the Corsi's Block Test.

Additionally, verbal memory (short-term and long-term) was investigated using the auditory verbal learning test (AVLT), while semantic memory was specifically explored using the naming to verbal description sub-test of the Sartori semantic battery. Visuospatial long-term memory was examined by the delayed recall of the Rey-Osterrieth complex figure (ROCF). The copy of ROCF further explored the patients' visuoconstructional abilities.

Attention and executive functions were assessed by administrating the Stroop test, The Trail Making Test A & B, and the Digit Span Backward.

In addition, we administered two further scales: the Depression, Anxiety, and Stress Scale − 21 Items (DASS-21) and the Modified Fatigue Impact Scale (MFIS). All raw scores were corrected by age and education, according to published norms, and performance was considered impaired if below the cut-off values.

2.4. MRI acquisition protocol

All participants underwent a standardized brain MRI acquisition protocol using a Siemens MAGNETOM Skyra 3T MR scanner equipped with a high-density head/neck array coil (64 channels).

The MRI protocol included high-resolution volumetric T1-weighted images (T1 MPRAGE, magnetization-prepared rapid gradient-echo, sagittal acquisition, isotropic voxel 1x1x1 mm^3, acquisition matrix

256x256, FOV 256 mm, repetition time TR = 2300 ms, echo time TE = 2.98 ms, inversion time TI = 900 ms, flip angle 9°, GRAPPA acceleration factor 2, acquisition time 5′21′′) and rs-fMRI (Gradient Echo – Echo Planar Imaging, GRE-*EPI*, isotropic voxel 2.5x2.5x2.5 mm^3, FOV 235 mm, repetition time TR = 735 ms, echo time TE = 37 ms, flip angle 53°, acquisition time 10 min).

2.5. Image pre-processing

The T1-weighted structural images were intensity-normalized and skull-stripped. Brain cortical and subcortical parcellation and segmentation were performed using FreeSurfer 6.0 (http://surfer.nmr.mgh.harvard.edu/).

A semi-automatic pipeline has been in- house developed for quality control of fMRI images: GRE-*EPI* volumes displaced>1.5 mm in one of the three spatial directions and rotated>1.5° around the three spatial axes with respect to the central volume of the temporal fMRI series were detected. A successive visual inspection was performed to define the number of volumes and the number of contiguous volumes characterized by this motion. The rs-fMR images were pre-processed following an in-house written standardized pipeline based on the FMRIB software library (FSL, https://fsl.fmrib.ox.ac.uk/fsl/fslwiki) with specific adjustments to these data. The steps included motion correction, phase-encoding distortions correction, brain extraction, spatial smoothing (using a 5 mm full width half maximum (FWHM, Gaussian filter), intensity normalization, high pass temporal filtering with a cut-off of 60 s, co-registration to T1-weighted structural images, registration to the standard Montreal Neurological Institute (MNI) space and manual independent component analysis-based data de-noising (Griffanti et al., 2017).

2.6. Morphometric analysis

Thirteen bilateral cortical and three subcortical regions of interest (ROIs) were selected from the FreeSurfer segmentation to match those regions typically associated with the functional olfactory network: anterior cingulate cortex, insular cortex (central, short, anterior, inferior, and superior circular), orbital cortex (inferior frontal, lateral, medial olfactory, H-shaped), rectus cortex, parahippocampal cortex, hippocampus, amygdala, thalamus (Lu et al., 2019; Tobia et al., 2016; Arnold et al., 2020; Seubert et al., 2013). The volume and the cortical thickness of such regions were extracted from the FreeSurfer output. Moreover, a neuroradiologist with>15 years of experience manually segmented the olfactory bulb on coronal view of the 3D T1-weighted MPRAGE volume (1 mm isotropic resolution, consistently acquired across all participants) in each subject using ITK-SNAP 3.8.0, and the region volume was evaluated separately for the left and right hemispheres.

Whole-brain voxel-based morphometry (VBM) was performed on the T1-weighted structural images using the SPM12 software (https://www.fil.ion.ucl.ac.uk/spm/software/spm12/). At first, the origin of all images was set close to the anterior commissure. The images were then segmented into grey matter, white matter, and CSF. The grey matter segmentations were iteratively registered to the group average to achieve the optimal deformation for their alignment. Finally, the original grey matter segmentations were Jacobian-scaled, registered to the MNI space through the template image generated at the previous step, and spatially smoothed with an 8 mm FWHM Gaussian filter.

2.7. Graph-based analysis of rs-fMRI

The pre-processed fMRI images were analysed with a graph-based approach, performed on Matlab R2020a, using the Brain Connectivity Toolbox (BCT) (Rubinov and Sporns, 2010) and the Network-Based Statistics (NBS) toolbox (Zalesky et al., 2010). Graph analysis is based on modelling the brain as a set of nodes, corresponding to ROIs, connected between each other through a set of links, whose strength describes the FC between the nodes. The ROIs were defined using the Brainnetome atlas (https://atlas.brainnetome.org/) (Fan et al., 2016), a connectivity-based parcellation of the human brain bilateral hemispheres into 246 regions. The average temporal series of the fluctuations of the BOLD signal within each ROI was extracted and each point of the time series was filtered using a Gaussian kernel, including the previous and the following point, to suppress high-frequency fluctuations. The FC among ROIs was calculated as the Pearson's correlation between each pair of time series. As their interpretation is debated, negative correlations were set to 0 (van den Heuvel et al., 2017). Fig. 1 shows a schematic representation of this process. The resulting FC matrix of each subject was then converted to normally distributed values using Fisher's r-to-Z transformation. The networks were then proportionally thresholded to create separate matrices in the range of 1–80 % of the strongest connections, with a step of 2 % (van den Heuvel et al., 2017). For each matrix generated following this procedure, a corresponding random matrix was created by permuting each link 10,000 times while preserving the global degree distribution for comparison and normalization of the global measures with the subject-derived matrices.

Several graph measures were evaluated at each threshold, both at the global and local level of the networks, aiming to characterize their properties of integration, segregation, cliquishness, and nodal centrality (Rubinov and Sporns, 2010). At the global level, the measures included the global efficiency and the characteristic path length (integration measures), the average clustering coefficient, the average local efficiency, and the modularity coefficient (segregation measures). The modules were independently identified at each threshold through the community Louvain algorithm. Moreover, the small-worldness, a property that combines both segregation and integration information, was calculated. At the local level, the local efficiency, the clustering coefficient and the within-module Z-score (cliquishness measures), the degree, the strength and the betweenness centrality (centrality measures), and the participation coefficient (integration measure) were evaluated. All the properties were then integrated over a density range of 5–50 %, i.e., the interval where the networks demonstrated small-world properties, characteristic of brain graphs (Bullmore and Bassett, 2011).

Additionally, NBS was used to identify topological clusters of altered connectivity between the FC graphs of patients and controls. This approach was applied in the 5–50 % density range, to potentially reveal sub-networks of altered connectivity at different levels. To summarize the results, a score was assigned to each altered link and set equal to the frequency of significant alteration (i.e., the number of density levels at which the link was altered over the density range), weighted by the normalized inverse p-value assigned to the cluster by NBS.

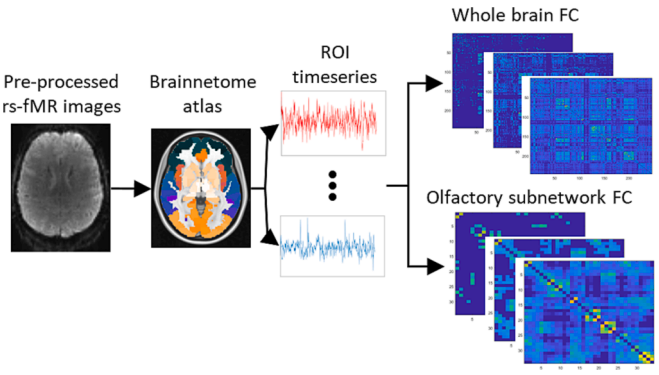

Fig. 1. Image processing pipeline: the pre-processed rs-fMR images were registered to the MNI standard space, where the Brainnetome regions of interest (ROIs) were defined. The time series of each ROI was extracted and the Pearson's correlation between each pair of ROIs was calculated to generate one functional connectivity (FC) matrix per subject, at different thresholds. The same procedure was followed for the whole brain and the olfactory subnetwork.

Alongside the whole-brain graphs, a subgraph corresponding to the olfactory network was also defined by selecting a subset of 25 bilateral ROIs among the 246 provided by the Brainnetome atlas to match the functional olfactory graph defined by Arnold and colleagues (Arnold et al., 2020). Since there was no direct correspondence between the Brainnetome ROIs and the reference regions, the thalamus and amygdala ROIs of the atlas were merged into a single component to obtain the best match. Moreover, the anterior and rostral cingulate gyri were included as additional ROIs, based on the information provided by the existing literature about the functional olfactory network (Lu et al., 2019; Tobia et al., 2016; Seubert et al., 2013). The final olfactory subnetwork included 34 nodes (17 per hemisphere), represented in Fig. 2.

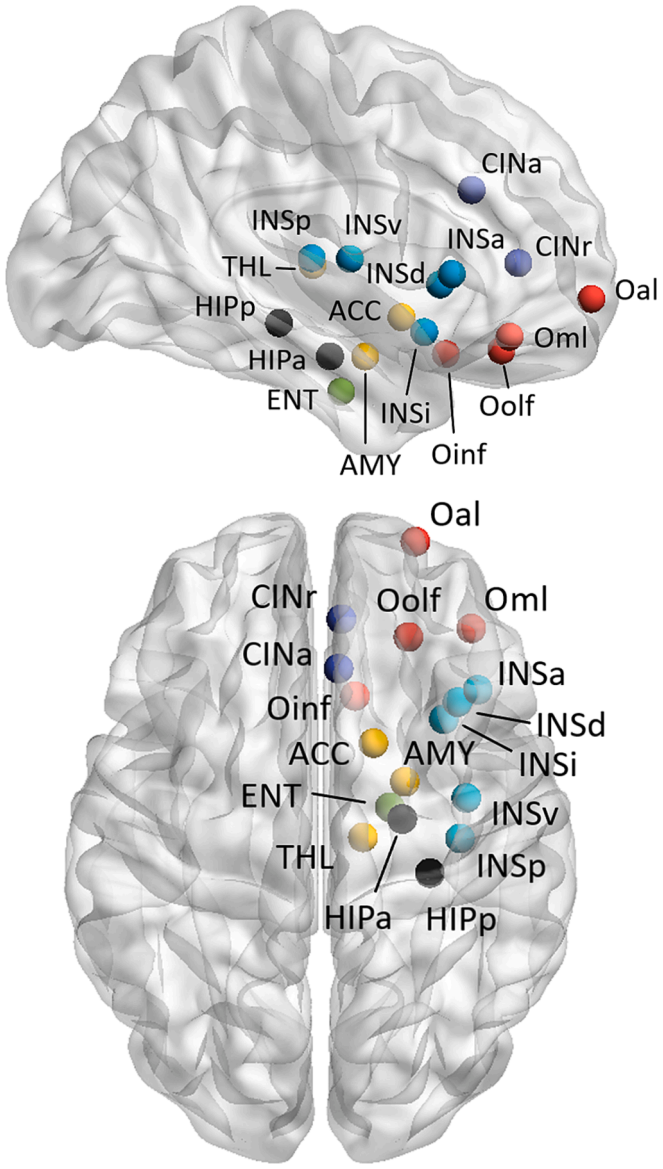

Fig. 2. Representation of the nodes selected to build the olfactory subnetwork in axial and sagittal views. For readability, the nodes are shown only in the right hemisphere, even though all the regions were considered bilaterally. Red: olfactory cortex; blue: cingulate cortex; light blue: insula; yellow: basal ganglia, black: hippocampus; green: entorhinal cortex. ACC, nucleus accumbens; AMY, amygdala; CINa, anterior cingulate gyrus; CINr, rostral cingulate gyrus; *ENT*, entorhineal cortex; HIPa, anterior hippocampus; HIPp, posterior hippocampus; INSa, anterior insula; INSd, dorsal insula; INSi, inferior anterior insula; INSp, posterior insula; INSv, ventral insula; Oal, anterior lateral orbitofrontal cortex; Oinf, inferior orbital cortex; Oml, medial lateral orbitofrontal cortex; Oolf, orbital olfactory cortex; THL, thalamus.

2.8. Correlation analysis

The patients' features of the FC graphs that resulted significantly altered compared with controls were exploratively correlated with the scores of the Sniffin' Sticks test and with an *a priori* chosen subset of neuropsychological cognitive and psychological scales. For this purpose, we used Pearson's correlation analysis. Furthermore, Pearson's correlations were performed between all variables to assess the association between the Sniffin' Sticks test scores and neuropsychological performance.

2.9. Statistical analysis

The volumetric and cortical thickness data were corrected for the estimated total intracranial volume (eTIV). A *t*-test was used to look for alterations in these regions after checking for the normal distribution of the parameters. The Bonferroni method was used to correct for multiple comparisons.

For the VBM analysis, the statistical significance of group differences was assessed through nonparametric permutation with the Randomise tool of FSL. The eTIV was added as a nuisance regressor in the design, and the threshold-free cluster enhancement (TFCE) option was set to identify cluster-like structures. Family-wise error rate (FWER) was used to correct for multiple comparisons.

The results obtained for each FC graph measure were compared between patients and controls using analysis of covariance (ANCOVA) and age as a covariate regressor to investigate the existence of alterations between the two groups. The analysis was also repeated to account for sex differences. The Bonferroni method was adopted to account for multiple comparisons.

For NBS, a mass univariate *t*-test on all graph edges with a threshold of 3.1 was used to identify the altered links, followed by FWER to control for multiple comparisons.

Statistical significance was set at p-value < 0.05 after correction for multiple comparisons.

2.10. Standard protocol approvals, registrations, and patient consent

This study was approved by the local institutional review board (reference number: 853–2021-SPER-AUSLBO). Written informed consent was obtained from all participants in the study.

3. Results

3.1. Study population

A total of 23 patients presenting with persistent COVID-19-related OD underwent olfactory assessment, neuropsychological, and MRI evaluation. The clinical features and results of the olfactory evaluation for each patient are summarized in Table 1. The mean age was 37 ± 14 years, and 12 (52 %) were females. Twenty (87 %) patients had mild acute COVID-19, not requiring hospitalization, while among the three hospitalized patients, only one developed life-threatening complications, including COVID-19-related encephalopathy. All patients were infected prior to May 2021. There were no significant comorbidities to report.

Twenty-six healthy controls (mean age 38.5 ± 13.7 years, range 21–63 years, 13 females), who did not report any olfactory, cognitive or neurological dysfunction, underwent the same MRI protocol as the OD cohort.

3.2. Olfactory function assessment (patients only)

The mean duration of OD was 11 ± 5 months, ranging from 2 to 19 months. Of note, the single patient tested when the symptom duration was < 3 months (ID 14) meets long COVID criteria according to

Table 1
Clinical features and olfactory function assessment.

ID	Age (y), Sex	Hospitalization	OD duration (mo)	Associated dysosmia/gustatory dysf.	T (n/16)	D (n/16)	I (n/16)	Total (n/48)
1	47, M	No	8	Yes / No	11.25	11	8	30.25
2	71, M	Yes	14	No / Yes	3.75	8	9	20.75
3	35, M	No	12	Yes / Yes	4.5	10	6	20.5
4	25, M	No	6	Yes / Yes	3.5	11	10	24.5
5	30, M	Yes	15	Yes / Yes	5	11	13	29
6	30, F	No	16	No / Yes	0	6	4	10
7	52, F	No	10	No / Yes	5.5	11	7	23.5
8	24, F	No	9	No / Yes	3.75	10	6	19.75
9	37, F	No	11	No / Yes	7.25	11	10	28.25
10	41, F	No	6	No / Yes	6.25	12	12	30.25
11	36, F	No	18	No / Yes	1	11	8	20
12	14, F	No	8	Yes / Yes	1	11	9	21
13	55, M	No	10	Yes / Yes	7.75	12	11	30.75
14	28, F	No	2	Yes / Yes	8	14	12	34
15	24, M	No	19	No / Yes	5.5	7	8	20.5
16	64, F	No	18	No / Yes	2.75	10	8	20.75
17	29, F	No	10	No / Yes	6.5	7	8	21.5
18	33, M	No	7	Yes / Yes	8.5	11	10	29.5
19	19, F	No	12	No / No	2.5	11	10	23.5
20	23, M	No	5	Yes / Yes	5.5	12	11	28.5
21	53, M	No	6	No / No	3	12	11	26
22	30, M	No	17	Yes / Yes	6	12	10	28
23	46, F	Yes	7	No / No	4.75	10	11	25.75

OD, olfactory dysfunction; T, olfactory threshold; D, odor discrimination; I, odor identification.

Nalbandian et al. (2021)) but not WHO (Post COVID-19 condition (Long COVID), Accessed March 8, 2023). At the time of testing, all patients reported a quantitative olfactory defect associated with dysosmia in 10 (43 %) cases (cacosmia, n = 7, phantosmia, n = 1, parosmia, n = 3) and persistent gustatory dysfunction in 19 (83 %).Nine patients had both dysosmia and gustatory dysfunction. The mean TDI score at Sniffin' Sticks test was 23.63 ± 5.32 points: one patient had functional anosmia, 21 patients had hyposmia, and one patient had normosmia (scoring 30.75, the cut-off value), with concomitant dysosmia and gustatory dysfunction.

3.3. Neuropsychological evaluation (patients only)

Mean neuropsychological raw and corrected scores, and the percentage of pathological values are reported for all patients (N = 23) in Table 2.

Memory and executive functions were the two cognitive domains mainly impaired. Specifically, short-term and long-term verbal memory were impaired in 9 % and 13 % of patients, while short-term and long-term visuospatial memory were impaired in 9 % and 17 % of patients. Moreover, regarding the executive function domain, deficits in the ability to inhibit cognitive interference and working memory deficits were found respectively in 10 % and 13 % of patients.

Almost one-third of the patients had a pathological depression score, while three-fourth of patients had a pathological fatigue score.

Significant correlations were found between odor discrimination and executive function abilities: attentive abilities (i.e., Trail Making Test A) ($r = -0.631$, $p = 0.001$) and cognitive flexibility (i.e., Trail Making Test B) ($r = -0.768$, $p < 0.001$).

3.4. Morphometric analysis (patients vs controls)

The cortical thickness of the selected regions did not show any significant alteration between patients and controls.

The volumes of the left lateral orbital cortex ($p = 0.034$) and the bilateral hippocampus (left: $p = 0.003$, right: $p = 0.002$) and amygdala (left: $p = 0.023$, right: $p = 0.014$) exhibited a significant reduction in patients, which however did not survive to statistical correction for multiple comparisons. The manually segmented olfactory bulb volumes did not differ significantly between patients and controls and were symmetrical between the left and right hemispheres.

The VBM revealed trending alterations of local grey matter concentration in the superior frontal cortex, which again were not significant after the correction for multiple comparisons.

3.5. Functional graph analysis (patients vs controls)

3.5.1. Whole-brain

Four rs-fMRI sequences of patients were excluded from the analysis due to movement image artifacts; therefore, 45 sequences underwent further examination (19 in the OD cohort, 26 controls). From the whole-brain graph analysis, no significant alterations emerged at the global nor local level; trends of alterations in terms of nodal centrality and efficiency were observed in the basal ganglia, particularly in the thalamus and putamen. However, such differences did not maintain statistical significance after the correction for multiple comparisons. Similarly, sub-clusters of significantly altered connectivity were not identified through NBS.

3.5.2. Olfactory subnetwork

When restricting the analysis to the olfactory sub-network, statistically significant alterations were detected both at the global and local levels in patients. The global modularity coefficient was significantly reduced in patients compared to controls ($p = 0.03$), indicating that long-COVID patients exhibited a sub-network structure with less closely segregated clusters than controls.

Moreover, local alterations of the centrality of the right thalamus were discovered, notably an increase of both the number (degree, $p = 0.0008$) and the strength ($p = 0.0003$) of the connections (Fig. 3, *Supplementary* Fig. 1). These results overcame the correction for multiple comparisons with Bonferroni. Results accounting for sex differences are reported in Supplementary Fig. 2.

The links driving the altered connectivity within the olfactory network were investigated through NBS, which, after FWER correction, revealed the existence of similar clusters of increased FC in patients at different network densities.All the clusters were centered in the right thalamus and included several ROIs, mostly belonging to the ipsilateral hemisphere. The altered connections are shown in Fig. 4, where the link thickness correspond to its significance score. The edge connecting the right thalamus with the right posterior hippocampus was the most

Table 2
Neuropsychological assessment.

		Raw Score (mean)	sd	Corrected Score (mean)	sd	normal values cut offs	% pathological scores (Including only equivalent scores = 0)
	Age (years)			37,4	14,42		
	Education (years)			16	3,06		
	Sex (M/F)			11/12			
	Clinical Tests						
Cognitive screening	MoCA score	25.74	2.51	25.74	2.51	≥ 18.29	4 %
Attention and Executive functions	Digit Span Backward	4.39	1.03	3.83	1.08	≥3.29	13 %
	Stroop test (RT-*sec*)	13.10	6.89	22.77	7.24	≤36.91	10 %
	Stroop test (Error)	0.29	0.90	3.25	1.15	≤4.23	5 %
	TMT_A	34.74	13.41	42.30	15.28	≤93 *sec.*	0 %
	TMT_B	88.22	30.69	119.55	42.38	≤282 *sec.*	0 %
Verbal memory	AVLT_immediate recall	49.26	11.16	41.69	9.30	≥28.53	9 %
	AVLT_delayed recall	10.09	3.41	7.76	3.13	≥4.69	13 %
	Naming to verbal description_animate	7.91	0.42	7.91	0.42	≥4.46	0 %
	Naming to visual description_animate	7.17	0.94	7.17	0.94	≥3.61	0 %
	Naming to verbal description_concrete inanimate	8.87	0.87	8.87	0.87	≥7.33	0 %
	Naming to verbal description_abstract inanimate	9.13	0.69	9.13	0.69	≥6.69	0 %
	Digit Span Forward	6.13	0.87	5.51	0.83	≥3.75	0 %
Visuo-spatial memory	Corsi's Block Test	5.13	1.22	4.63	1.08	≥3.75	9 %
	ROCF_delayed recall	21.24	6.59	17.35	6.01	≥9.47	17 %
Language	Associative Fluency Test	40.13	12.79	32.17	12.19	≥17.35	4 %
	Category Words Fluency Test	50.57	9.94	44.87	9.37	≥25	0 %
Visuoconstructional abilities	ROCF_copy	33.76	3.56	32.51	4.27	≥28.88	4 %
Depression, anxiety and stress	DASS-21Depression score	5.65	4.82	5.65	4.82	≤9	30 %
	DASS-21Anxiety score	5.09	3.42	5.09	3.42	≤7	13 %
	DASS-21Stress score	8.22	4.88	8.22	4.88	≤14	17 %
Fatigue	MFIS_Total score	35.00	20.12	35.00	20.12	>12.3	74 %
	MFIS_Physical score	15.00	10.90	15.00	10.90	>2.4	74 %
	MFIS_Cognitive score	16.52	8,92	16.52	8.92	>3.5	83 %
	MFIS_Psychosocial score	3.48	3.76	3.48	3.76	>6.4	4 %

Table 2 presents raw and corrected neuropsychological data availables for 23 patients. Normal cut-off values are also presented along with the patients' ratio of pathological scores (deficitary and borderline scores). MoCA: Montreal Cognitive Assessment; RT-*sec*: Reaction time, seconds; AVLT: auditory verbal learning test; ROCF: Rey-Osterrieth complex figure; TMT: Trail Making Test; DASS: Depression, Anxiety and Stress Scale; MFIS: Modified Fatigue Impact Scale.

significantly altered (score = 2.6, as defined in the Methods section), followed by connectivity with the right insula (score = 1.8).

3.6. Correlation analysis (patients only)

The exploratory correlation analysis with the clinical scores revealed that the global modularity coefficient of the olfactory network positively correlated with both threshold ($r = 0.61$, $p = 0.007$) and total scores ($r = 0.52$, $p = 0.028$) of the "Sniffin' Sticks" test. Moreover, significant negative correlations emerged between the strength of the connections of the right thalamus and two short-term verbal memory tests: the auditory verbal learning test immediate recall ($r = -0.55$, $p = 0.026$) and the description-based object naming ($r = -0.58$, $p = 0.016$). Fig. 5 summarizes these results.

4. Discussion

Our study was the first to explore both the neuropsychological profile and integrity of the olfactory system using brain morphometry and graph-based analysis of rs-fMRI in patients with COVID-19-related persistent OD. We detected alterations in the FC of the olfactory network that correlated with hyposmia severity and neuropsychological performance. No significant morphological alterations were found in patients compared with controls.

Hyposmia severity was objectively assessed with Sniffin' sticks test after almost one year from OD onset, a remarkably longer follow-up period compared with previous reports (Xydakis et al., 2021; Nalbandian et al., 2021). In addition to manifestations strictly associated with hyposmia, such as dysosmia and gustatory dysfunction, the most common accompanying symptom was fatigue, observed in three-fourths of cases, a percentage similar to that reported in other long-COVID cohorts

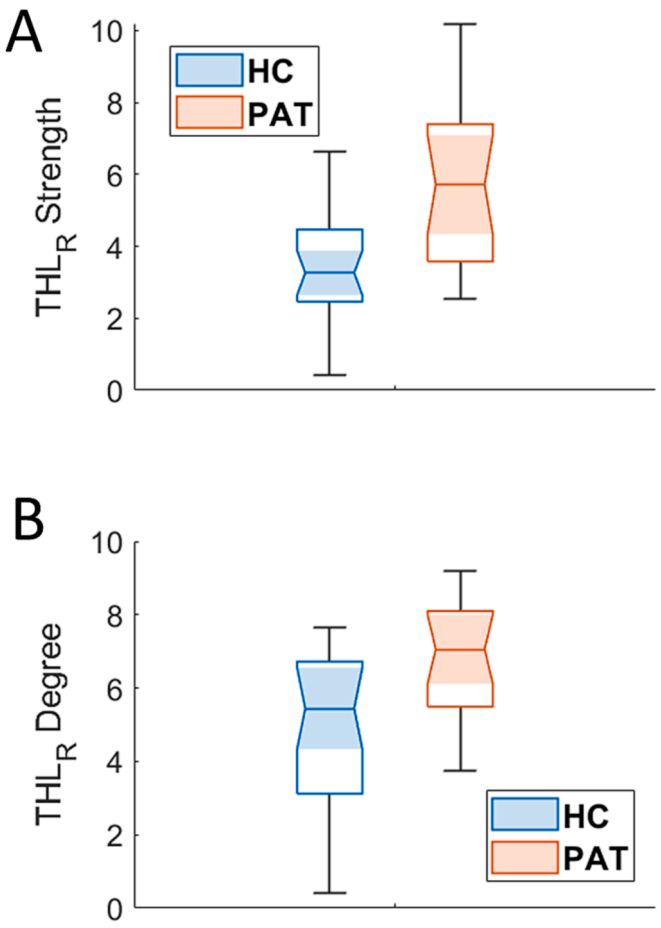

Fig. 3. Boxplot of strength (panel A) and degree (panel B) of the right thalamus in patients (red) and controls (light blue). The two quantities differed significantly between the two groups. HC, healthy controls; PAT, long-COVID; THLR, right thalamus.

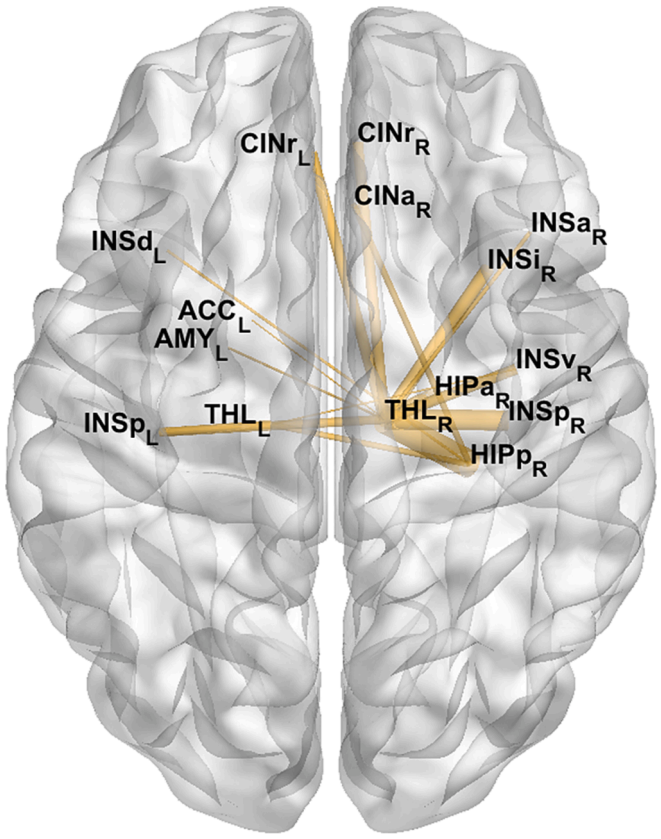

Fig. 4. Cluster of increased functional connectivity in patients within the olfactory network. The weights were assigned as the frequency over graph densities of the presence of altered connection, multiplied by the inverse p-value associated to the cluster at each density. The right thalamus constituted the center of this cluster, and its links with the right posterior hippocampus and insula were the most significantly altered.

(Tabacof et al., 2022; Huang et al., 2021). Less than one-fifth of patients had impaired neuropsychological test scores. The cognitive areas most frequently affected were executive functions and visuospatial memory, in line with other studies focusing on the long-term neuropsychological effects of COVID-19 (Llana et al., 2022; Hall et al., 2022; Ferrucci et al., 2022). Notably, neuropsychological deficits have been associated with alterations in brain functional connectivity in a previous study (Voruz et al., 2023). Most patients in our cohort had a mild disease course, as only 3/23 required hospitalization during acute COVID-19. Accordingly, even young people with mild acute disease can develop long-COVID neuropsychiatric manifestations, including hyposmia, cognitive dysfunction, and fatigue (Nalbandian et al., 2021; Spudich and Nath, 2022; Lechien et al., 2020).

The morphometric analysis of the olfactory network did not show any significant alteration in patients compared to controls after correction for multiple comparisons. However, the volumes of the left lateral orbital cortex, bilateral hippocampus, and amygdala exhibited a reduction trend in the OD cohort. Interestingly, Douaud et al. showed that subjects with previous COVID-19 had significantly greater atrophy in these and other cortical areas connected to primary olfactory cortices compared with pre-infection findings and controls, although in that study olfactory function was not investigated (Douaud et al., 2022). The reduction trend in volume observed in our long-COVID cohort may have emerged more significantly with a larger cohort of patients.

Similarly to Douad et al., we did not find any difference in the volumes of the manually segmented olfactory bulb between patients and controls. Contrastingly, a few previous neuroimaging reports described olfactory bulb atrophy and signal abnormalities in patients with COVID-19-related OD (Keshavarz et al., 2021; Yildirim et al., 2022), findings consistent with those of an autoptic study showing axon injury and microvasculopathy in the olfactory tissue (Ho et al., 2022). These discrepancies among neuroimaging studies may be explained by the localization of the olfactory bulbs in a region above the sinuses prone to susceptibility distortions and difficulties in segmenting MRI data (Douaud et al., 2022).

We employed graph analysis to examine the functional integrity of the olfactory system.

No significant alterations emerged in the whole-brain graph analysis at the global level. At the same time, nodal centrality and efficiency in subcortical nuclei showed trends of alterations, not significant following correction for multiple comparisons. The most exciting findings emerged from analysing the olfactory network's global and local properties. In patients with COVID-19-related OD, the global modularity coefficient was significantly reduced compared with controls and showed a positive correlation with the threshold and total score of the olfactory assessment with the Sniffin' Sticks test. Modularity represents a measure of segregation, reflecting the degree to which a network is organized into a modular structure, i.e., a set of closely intra-connected clusters, a highly preserved characteristic of neuronal networks (Newman, 2006) Thus, the olfactory network of patients with COVID-19-related OD was overall less segregated into clusters of functionally associated components, which likely play specific functions in the central olfactory processing. As suggested by the correlation of segregation impairment with hyposmia severity, the reduced modularity of the olfactory network reflects a lower performance of the network itself,

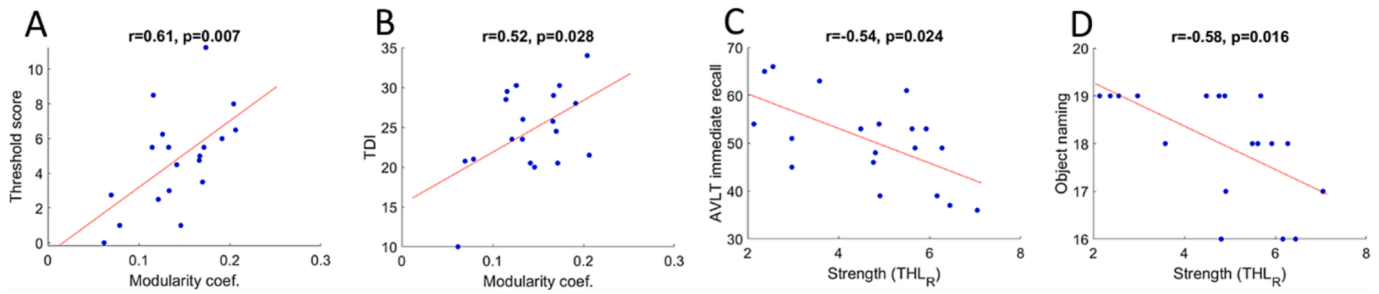

Fig. 5. Results emerging from Pearson's correlations between the significantly altered functional graph properties of the olfactory network and the clinical scales. The modularity coefficient was found to have a significant positive relationship with the threshold (panel A) and the total scores (panel B) of the Sniffin' Sticks test, while the strength of the connections of the right thalamus showed a negative relation with short-term memory tests (panels C, D). AVLT, auditory verbal learning test; NPS, neuropsychological assessment.

similarly to what has been shown for the whole-brain connectivity and cognition (Bertolero et al., 2018). To our knowledge, no other study evaluated the modularity structure of FC graphs in the long-COVID population; however, a reduced modularity coefficient, at the whole brain level, associated to disease severity has been found in patients with post-traumatic anosmia (Park et al., 2019). Regarding local properties of the olfactory network, we detected alterations of the centrality of the right thalamus in the OD-cohort, concerning an increase of both the degree and strength of the connections, which was inversely correlated with the performance in short-term verbal memory tests.

A distinctive feature of the olfactory system is the absence of primary connections with the thalamus, since the axons of olfactory bulb neurons project directly to the primary olfactory cortices (Shepherd, 2005). However, these are strictly connected to the thalamus via the so-called indirect pathway (Ongur, 1991; Milardi et al., 2017), which, along with the direct pathway, projects odorant information to the orbitofrontal cortex and is involved in the conscious perception of odors (Milardi et al., 2017). Indeed, several lesion studies in rats followed by more recent human studies suggest a role of the thalamus in functions ranging from olfactory perception to attention (Eichenbaum et al., 1980; Sela et al., 2009; McBride and Slotnick, 1997; Ridley et al., 2005). Notably, Sela et al. showed that only right thalamic lesions altered olfactory hedonics of pleasant odors (Sela et al., 2009), which may be speculatively related to dysosmia/cacosmia, reported by 43 % of our patients. Additionally, we found that the edge connecting the right thalamus with the right posterior hippocampus was the most significantly increased, and a negative correlation was found between the strength of the right thalamus and short-term verbal memory tests, suggesting a compensatory mechanism. As the hippocampal-thalamic interactions represent an interdependent system vital for episodic memory (Aggleton et al., 2010), dysfunctional thalamic connectivity might be related with memory impairment that we detected in our COVID 19 patients. Moreover, this observation remarks anatomical overlap between the olfactory and memory networks (Insausti et al., 2002). Altered connectivity of subcortical structures has recently been associated with memory scores in a group of long-COVID patients (6–9 months) (Voruz et al., 2023); however, in this group, the patients did not necessarily showed OD, but were rather stratified based on the hospitalization at the time of the infection.

A recently published work by Esposito et al. (Esposito et al., 2022) used a graph-based approach to analyse the rs-fMRI of patients with COVID-19-related OD, studied within 3 weeks after returning SARS-CoV-2 free. However, the authors focused on the characterization of the FC of the anterior piriform cortex, showing an increased local connectivity (Esposito et al., 2022), whereas our analysis aimed to provide a broader, comprehensive description of the whole-brain and functional olfactory networks. In addition to the large difference of follow-up duration, much longer in our study, the distinct definition of nodes chosen to construct the graphs does not allow a direct comparison with our findings. Nodes were constructed as 4 mm radius spheres by Esposito and colleagues, whereas they were extracted as ROIs from the Brainnetome atlas in our study, the latter not including a ROI of the anterior piriform cortex. The ROI defined by Esposito and colleagues would overlap a small portion of the inferior orbital cortex, orbital olfactory cortex, and inferior anterior insula, while having a significantly smaller volume with respect to each of them. Despite these differences, both studies support the hypothesis of functional involvement of the central olfactory system in COVID-19-related short- and long-term OD. Interestingly, the olfactory network has also been shown to have a higher connectivity with the default mode network in long COVID (Zhang et al., 2022).

The mechanisms underlying the observed alterations in the FC of the olfactory network are yet to be elucidated but may represent a consequence of the loss of sensory input due to anosmia, neuroinflammatory events, or neurodegeneration. Although a pathogenic role of direct SARS-CoV-2 neuroinvasion via uptake by olfactory neuronal terminals has been suggested (Xydakis et al., 2021), most studies agree that SARS-CoV-2 brain invasion occurs in only a small fraction of cases, as SARS-CoV-2 gene sequences have been detected only in a minority of subjects (Serrano et al., 2022).

In several neurodegenerative conditions, notably Parkinson's disease and Alzheimer's disease, OD represents a prodromal manifestation appearing years before the overt motor and cognitive symptoms (Ongur, 1991) The underlying pathogenic mechanisms have not been fully understood yet, but it has been hypothesized that a common primordial neuropathological substrate may exist (Doty, 2017).

Together with others describing the neuropsychological sequelae (Hall et al., 2022; Ferrucci et al., 2022) and the degenerative changes in limbic brain regions (Douaud et al., 2022), our findings raise the alarming possibility that long-term consequences of SARS-CoV-2 infection might contribute to neurodegeneration. Regarding olfactory function, a 2-year follow-up study showed that over 60 % of patients with COVID-19-related OD did not experience a complete recovery (McWilliams et al., 2022). Preliminary studies showed that olfactory rehabilitation and oral supplementation with palmitoylethanolamide and luteolin may facilitate the recovery process (Lechien et al., 2023; Di Stadio et al., 2022).

A key question is whether the neurodegenerative changes might be reversed, stabilized, or progress. The answer will come from follow-up studies and is of utmost importance considering the unprecedented diffusion of the COVID-19 pandemic.

4.1. Limitations

An important limitation of the current study is that we could not perform olfactory and neuropsychological evaluations in the control cohort. However, unlike long-COVID patients, the controls did not report any cognitive or olfactory impairment, yet we cannot exclude with certainty subtle, subclinical alterations. Moreover, all patients were infected prior to May 2021, limiting the validity of our observations to

the first SARS-CoV-2 variants.

The relatively small number of included patients may have reduced the statistical significance of some of the described findings, notably in the morphometric analysis.

From the technical perspective, a further limitation is that GR-*EPI* sequences are known to be affected by susceptibility distortions in the phase-encoding direction; as a consequence, the raw images presented artifacts especially in the rostral medial frontal area. Even though these artifacts were corrected at the pre-processing step following standardized procedures, they may still affect the signal integrity in such areas.

Finally, as this is the first paper to provide a complete graph-based functional characterization of the whole-brain and olfactory networks in long-COVID patients, future brain connectivity studies with larger sample sizes are needed to confirm or expand our findings, possibly also by adopting other methods of nodes selection.

4.2. Conclusion

Less than one-fifth of patients with COVID-19-related persistent OD showed neuropsychological deficits, predominant in executive functions and memory. Despite the absence of significant morphological alterations, graph-based analysis of rs-fMRI detected alterations of the olfactory subnetwork functional connectivity, correlated with hyposmia severity and neuropsychological performance. Considering the alarming evidence suggesting neurodegeneration in long-COVID patients, further studies are critically needed in order to elucidate the pathomechanism and the long-term evolution of this condition.

CRediT authorship contribution statement

Lorenzo Muccioli: Conceptualization, Data curation, Writing – original draft. **Giovanni Sighinolfi:** Data curation, Writing – original draft. **Micaela Mitolo:** Conceptualization, Data curation, Writing – original draft. **Lorenzo Ferri:** Conceptualization, Data curation, Writing – original draft. **Magali Jane Rochat:** Conceptualization, Data curation, Writing – original draft. **Umberto Pensato:** Conceptualization, Data curation. **Lisa Taruffi:** Data curation. **Claudia Testa:** Data curation. **Marco Masullo:** Data curation. **Pietro Cortelli:** Data curation. **Raffaele Lodi:** Data curation. **Rocco Liguori:** Data curation. **Caterina Tonon:** Conceptualization, Data curation. **Francesca Bisulli:** Conceptualization, Data curation.

Declaration of Competing Interest

The authors declare that they have no known competing financial interests or personal relationships that could have appeared to influence the work reported in this paper.

Data availability

Data will be made available on request.

Appendix A. Supplementary data

Supplementary data to this article can be found online at https://doi.org/10.1016/j.nicl.2023.103410.

References

Aggleton, J.P., O'Mara, S.M., Vann, S.D., Wright, N.F., Tsanov, M., Erichsen, J.T., 2010. Hippocampal-anterior thalamic pathways for memory: uncovering a network of direct and indirect actions. Eur J Neurosci. 31 (12), 2292–2307. https://doi.org/10.1111/j.1460-9568.2010.07251.x.

Arnold, T.C., You, Y., Ding, M., Zuo, X.N., de Araujo, I., Li, W., 2020. Functional Connectome Analyses Reveal the Human Olfactory Network Organization. eneuro. 7 (4):ENEURO.0551-19.2020 https://doi.org/10.1523/ENEURO.0551-19.2020.

Barletta-Rodolfi, C., Gasparini, F., Ghidoni, E., 2011. Kit del neuropsicologo italiano. Published online, Bologna Soc Ital Neuropsicol.

Bertolero, M.A., Yeo, B.T.T., Bassett, D.S., D'Esposito, M., 2018. A mechanistic model of connector hubs, modularity and cognition. Nat Hum Behav. 2 (10), 765–777. https://doi.org/10.1038/s41562-018-0420-6.

Bullmore, E.T., Bassett, D.S., 2011. Brain Graphs: Graphical Models of the Human Brain Connectome. Annu Rev Clin Psychol. 7 (1), 113–140. https://doi.org/10.1146/annurev-clinpsy-040510-143934.

Capelli, S., Caroli, A., Barletta, A., Arrigoni, A., Napolitano, A., Pezzetti, G., Longhi, L.G., Zangari, R., Lorini, F.L., Sessa, M., Remuzzi, A., Gerevini, S., 2023. MRI evidence of olfactory system alterations in patients with COVID-19 and neurological symptoms. J Neurol. 270 (3), 1195–1206.

Cristillo, V., Pilotto, A., Cotti Piccinelli, S., et al., 2021. Age and subtle cognitive impairment are associated with long-term olfactory dysfunction after COVID-19 infection. J Am Geriatr Soc. 69 (10), 2778–2780. https://doi.org/10.1111/jgs.17296.

Di Stadio, A., D'Ascanio, L., Vaira, L.A., Cantone, E., De Luca, P., Cingolani, C., Motta, G., De Riu, G., Vitelli, F., Spriano, G., De Vincentiis, M., Camaioni, A., La Mantia, I., Ferreli, F., Brenner, M.J., 2022. Ultramicronized Palmitoylethanolamide and Luteolin Supplement Combined with Olfactory Training to Treat Post-COVID-19 Olfactory Impairment: A Multi-Center Double-Blinded Randomized Placebo-Controlled Clinical Trial. Curr Neuropharmacol. 20 (10), 2001–2012.

Doty, R.L., 2017. Olfactory dysfunction in neurodegenerative diseases: is there a common pathological substrate? Lancet Neurol. 16 (6), 478–488. https://doi.org/10.1016/S1474-4422(17)30123-0.

Douaud, G., Lee, S., Alfaro-Almagro, F., Arthofer, C., Wang, C., McCarthy, P., Lange, F., Andersson, J.L.R., Griffanti, L., Duff, E., Jbabdi, S., Taschler, B., Keating, P., Winkler, A.M., Collins, R., Matthews, P.M., Allen, N., Miller, K.L., Nichols, T.E., Smith, S.M., 2022. SARS-CoV-2 is associated with changes in brain structure in UK Biobank. Nature 604 (7907), 697–707. Published online.

Eichenbaum, H., Shedlack, K.J., Eckmann, K.W., 1980. Thalamocortical mechanisms in odor-guided behavior. I. Effects of lesions of the mediodorsal thalamic nucleus and frontal cortex on olfactory discrimination in the rat. Brain Behav Evol. 17 (4), 255–275. https://doi.org/10.1159/000121803.

Esposito, F., Cirillo, M., De Micco, R., et al., 2022. Olfactory loss and brain connectivity after COVID-19. Hum Brain Mapp. 43 (5), 1548–1560. https://doi.org/10.1002/hbm.25741.

Evangelisti, S., Testa, C., Ferri, L., Gramegna, L.L., Manners, D.N., Rizzo, G., Remondini, D., Castellani, G., Naldi, I., Bisulli, F., Tonon, C., Tinuper, P., Lodi, R., 2018. Brain functional connectivity in sleep-related hypermotor epilepsy. NeuroImage Clin. 17, 873–881.

Evangelisti, S., Pittau, F., Testa, C., Rizzo, G., Gramegna, L.L., Ferri, L., Coito, A., Cortelli, P., Calandra-Buonaura, G., Bisquoli, F., Bianchini, C., Manners, D.N., Talozzi, L., Tonon, C., Lodi, R., Tinuper, P., 2019. L-Dopa Modulation of Brain Connectivity in Parkinson's Disease Patients: A Pilot EEG-fMRI Study. Front Neurosci. 13 https://doi.org/10.3389/fnins.2019.00611.

Fan, L., Li, H., Zhuo, J., Zhang, Y.u., Wang, J., Chen, L., Yang, Z., Chu, C., Xie, S., Laird, A.R., Fox, P.T., Eickhoff, S.B., Yu, C., Jiang, T., 2016. The Human Brainnetome Atlas: A New Brain Atlas Based on Connectional Architecture. Cereb Cortex. 26 (8), 3508–3526.

Farahani, F.V., Karwowski, W., Lighthall, N.R., 2019. Application of Graph Theory for Identifying Connectivity Patterns in Human Brain Networks: A Systematic Review. Front Neurosci. 13, 585. https://doi.org/10.3389/fnins.2019.00585.

Ferrucci, R., Dini, M., Rosci, C., Capozza, A., Groppo, E., Reitano, M.R., Allocco, E., Poletti, B., Brugnera, A., Bai, F., Monti, A., Ticozzi, N., Silani, V., Centanni, S., D'Arminio Monforte, A., Tagliabue, L., Priori, A., 2022. One-year cognitive follow-up of COVID-19 hospitalized patients. Eur J Neurol 29 (7), 2006–2014. Published online.

Graham, E.L., Clark, J.R., Orban, Z.S., Lim, P.H., Szymanski, A.L., Taylor, C., DiBiase, R. M., Jia, D.T., Balabanov, R., Ho, S.U., Batra, A., Liotta, E.M., Koralnik, I.J., 2021. Persistent neurologic symptoms and cognitive dysfunction in non-hospitalized Covid-19 "long haulers". Ann Clin Transl Neurol. 8 (5), 1073–1085.

Griffanti, L., Douaud, G., Bijsterbosch, J., Evangelisti, S., Alfaro-Almagro, F., Glasser, M. F., Duff, E.P., Fitzgibbon, S., Westphal, R., Carone, D., Beckmann, C.F., Smith, S.M., 2017. Hand classification of fMRI ICA noise components. Neuroimage 154, 188–205.

Hall, P.A., Meng, G., Hudson, A., Sakib, M.N., Hitchman, S.C., MacKillop, J., Bickel, W. K., Fong, G.T., 2022. Cognitive function following SARS-CoV-2 infection in a population-representative Canadian sample. Brain Behav Immun - Health. 21, 100454.

Ho, C.-Y., Salimian, M., Hegert, J., O'Brien, J., Choi, S.G., Ames, H., Morris, M., Papadimitriou, J.C., Mininni, J., Niehaus, P., Burke, A., Canbeldek, L., Jacobs, J., LaRocque, A., Patel, K., Rice, K., Li, L., Johnson, R., LeFevre, A., Blanchard, T., Shaver, C.M., Moyer, A., Drachenberg, C., 2022. Postmortem Assessment of Olfactory Tissue Degeneration and Microvasculopathy in Patients With COVID-19. JAMA Neurol 79 (6), 544.

Huang, C., Huang, L., Wang, Y., Li, X., Ren, L., Gu, X., Kang, L., Guo, L.i., Liu, M., Zhou, X., Luo, J., Huang, Z., Tu, S., Zhao, Y., Chen, L.i., Xu, D., Li, Y., Li, C., Peng, L. u., Li, Y., Xie, W., Cui, D., Shang, L., Fan, G., Xu, J., Wang, G., Wang, Y., Zhong, J., Wang, C., Wang, J., Zhang, D., Cao, B., 2021. 6-month consequences of COVID-19 in patients discharged from hospital: a cohort study. Lancet Lond Engl. 397 (10270), 220–232.

Insausti, R., Marcos, P., Arroyo-Jiménez, M.M., Blaizot, X., Martínez-Marcos, A., 2002. Comparative aspects of the olfactory portion of the entorhinal cortex and its projection to the hippocampus in rodents, nonhuman primates, and the human brain. Brain Res Bull. 57 (3–4), 557–560. https://doi.org/10.1016/s0361-9230(01)00684-0.

Ismail, I.I., Gad, K.A., 2021. Absent Blood Oxygen Level-Dependent Functional Magnetic Resonance Imaging Activation of the Orbitofrontal Cortex in a Patient With

Persistent Cacosmia and Cacogeusia After COVID-19 Infection. JAMA Neurol. 78 (5), 609. https://doi.org/10.1001/jamaneurol.2021.0009.
Kandemirli, S.G., Altundag, A., Yildirim, D., Tekcan Sanli, D.E., Saatci, O., 2021. Olfactory Bulb MRI and Paranasal Sinus CT Findings in Persistent COVID-19 Anosmia. Acad Radiol. 28 (1), 28–35. https://doi.org/10.1016/j.acra.2020.10.006.
Keshavarz, P., Haseli, S., Yazdanpanah, F., Bagheri, F., Raygani, N., Karimi-Galougahi, M., 2021. A Systematic Review of Imaging Studies in Olfactory Dysfunction Secondary to COVID-19. Acad Radiol. 28 (11), 1530–1540. https://doi.org/10.1016/j.acra.2021.08.010.
Kobal, G., Hummel, T., Sekinger, B., Barz, S., Roscher, S., Wolf, S., 1996. "Sniffin' sticks": screening of olfactory performance. Rhinology 34 (4), 222–226.
Larson, R.D., 2013. Psychometric Properties of the Modified Fatigue Impact Scale. Int J MS Care. 15 (1), 15–20. https://doi.org/10.7224/1537-2073.2012-019.
Lechien, J.R., Chiesa-Estomba, C.M., De Siati, D.R., Horoi, M., Le Bon, S.D., Rodriguez, A., Dequanter, D., Blecic, S., El Afia, F., Distinguin, L., Chekkoury-Idrissi, Y., Hans, S., Delgado, I.L., Calvo-Henriquez, C., Lavigne, P., Falanga, C., Barillari, M.R., Cammaroto, G., Khalife, M., Leich, P., Souchay, C., Rossi, C., Journe, F., Hsieh, J., Edjlali, M., Carlier, R., Ris, L., Lovato, A., De Filippis, C., Coppee, F., Fakhry, N., Ayad, T., Saussez, S., 2020. Olfactory and gustatory dysfunctions as a clinical presentation of mild-to-moderate forms of the coronavirus disease (COVID-19): a multicenter European study. Eur Arch Otorhinolaryngol. 277 (8), 2251–2261.
Lechien, J.R., Vaira, L.A., Saussez, S., 2023. Effectiveness of olfactory training in COVID-19 patients with olfactory dysfunction: a prospective study. Eur Arch Oto-Rhino-Laryngol Off J Eur Fed Oto-Rhino-Laryngol Soc EUFOS Affil Ger Soc Oto-Rhino-Laryngol - Head Neck Surg. 280 (3), 1255–1263. https://doi.org/10.1007/s00405-022-07665-4.
Llana, T., Mendez, M., Zorzo, C., Fidalgo, C., Juan, M.C., Mendez-Lopez, M., 2022. Anosmia in COVID-19 could be associated with long-term deficits in the consolidation of procedural and verbal declarative memories. Front Neurosci. 16, 1082811. https://doi.org/10.3389/fnins.2022.1082811.
Logue JK, Franko NM, McCulloch DJ, et al. Sequelae in Adults at 6 Months After COVID-19 Infection. *JAMA Netw Open*. 2021;4(2):e210830. doi:10.1001/jamanetworkopen.2021.0830.
Lovibond, P.F., Lovibond, S.H., 1995. The structure of negative emotional states: Comparison of the Depression Anxiety Stress Scales (DASS) with the Beck Depression and Anxiety Inventories. Behav Res Ther. 33 (3), 335–343.
Lu, Testa, Jordan, Elyan, Kanekar, Wang, Eslinger, Yang, Zhang, Karunanayaka, 2019. Functional Connectivity between the Resting-State Olfactory Network and the Hippocampus in Alzheimer's Disease. Brain Sci. 9 (12), 338.
McBride, S.A., Slotnick, B., 1997. The olfactory thalamocortical system and odor reversal learning examined using an asymmetrical lesion paradigm in rats. Behav Neurosci. 111 (6), 1273–1284. https://doi.org/10.1037//0735-7044.111.6.1273.
McWilliams, M.P., Coelho, D.H., Reiter, E.R., Costanzo, R.M., 2022. Recovery from Covid-19 smell loss: Two-years of follow up. Am J Otolaryngol. 43 (5), 103607 https://doi.org/10.1016/j.amjoto.2022.103607.
Milardi, D., Cacciola, A., Calamuneri, A., Ghilardi, M.F., Caminiti, F., Cascio, F., Andronaco, V., Anastasi, G., Mormina, E., Arrigo, A., Bruschetta, D., Quartarone, A., 2017. The Olfactory System Revealed: Non-Invasive Mapping by using Constrained Spherical Deconvolution Tractography in Healthy Humans. Front Neuroanat. 11 https://doi.org/10.3389/fnana.2017.00032.
Nalbandian, A., Sehgal, K., Gupta, A., Madhavan, M.V., McGroder, C., Stevens, J.S., Cook, J.R., Nordvig, A.S., Shalev, D., Sehrawat, T.S., Ahluwalia, N., Bikdeli, B., Dietz, D., Der-Nigoghossian, C., Liyanage-Don, N., Rosner, G.F., Bernstein, E.J., Mohan, S., Beckley, A.A., Seres, D.S., Choueiri, T.K., Uriel, N., Ausiello, J.C., Accili, D., Freedberg, D.E., Baldwin, M., Schwartz, A., Brodie, D., Garcia, C.K., Elkind, M.S.V., Connors, J.M., Bilezikian, J.P., Landry, D.W., Wan, E.Y., 2021. Post-acute COVID-19 syndrome. Nat Med. 27 (4), 601–615.
Newman, M.E.J., 2006. Modularity and community structure in networks. Proc Natl Acad Sci U S A. 103 (23), 8577–8582. https://doi.org/10.1073/pnas.0601602103.
Oldfield, R.C., 1971. The assessment and analysis of handedness: The Edinburgh inventory. Neuropsychologia 9 (1), 97–113. https://doi.org/10.1016/0028-3932(71)90067-4.
Oleszkiewicz, A., Schriever, V.A., Croy, I., Hähner, A., Hummel, T., 2019. Updated Sniffin' Sticks normative data based on an extended sample of 9139 subjects. Eur Arch Otorhinolaryngol. 276 (3), 719–728. https://doi.org/10.1007/s00405-018-5248-1.
Ongür D, Price JL. The organization of networks within the orbital and medial prefrontal cortex of rats, monkeys and humans. *Cereb Cortex N Y N 1991*. 2000;10(3):206-219. doi:10.1093/cercor/10.3.206.
Park, M., Chung, J., Kim, J.K., Jeong, Y., Moon, W.J., 2019. Altered Functional Brain Networks in Patients with Traumatic Anosmia: Resting-State Functional MRI Based on Graph Theoretical Analysis. Korean J Radiol. 20 (11), 1536. https://doi.org/10.3348/kjr.2019.0104.
Pirker-Kees, A., Platho-Elwischger, K., Hafner, S., Redlich, K., Baumgartner, C., 2021. Hyposmia Is Associated with Reduced Cognitive Function in COVID-19: First Preliminary Results. Dement Geriatr Cogn Disord. 50 (1), 68–73. https://doi.org/10.1159/000515575.
Post COVID-19 condition (Long COVID). Accessed March 8, 2023. https://www.who.int/europe/news-room/fact-sheets/item/post-covid-19-condition.
Ridley, R.M., Baker, H.F., Cummings, R.M., Green, M.E., Leow-Dyke, A., 2005. Mild topographical memory impairment following crossed unilateral lesions of the mediodorsal thalamic nucleus and the inferotemporal cortex. Behav Neurosci. 119 (2), 518–525. https://doi.org/10.1037/0735-7044.119.2.518.
Rubinov, M., Sporns, O., 2010. Complex network measures of brain connectivity: Uses and interpretations. Neuroimage 52 (3), 1059–1069. https://doi.org/10.1016/j.neuroimage.2009.10.003.
Sela, L., Sacher, Y., Serfaty, C., Yeshurun, Y., Soroker, N., Sobel, N., 2009. Spared and impaired olfactory abilities after thalamic lesions. J Neurosci Off J Soc Neurosci. 29 (39), 12059–12069. https://doi.org/10.1523/JNEUROSCI.2114-09.2009.
Serrano, G.E., Walker, J.E., Tremblay, C., Piras, I.S., Huentelman, M.J., Belden, C.M., Goldfarb, D., Shprecher, D., Atri, A., Adler, C.H., Shill, H.A., Driver-Dunckley, E., Mehta, S.H., Caselli, R., Woodruff, B.K., Haarer, C.F., Ruhlen, T., Torres, M., Nguyen, S., Schmitt, D., Rapscak, S.Z., Bime, C., Peters, J.L., Alevritis, E., Arce, R.A., Glass, M.J., Vargas, D., Sue, L.I., Intorcia, A.J., Nelson, C.M., Oliver, J., Russell, A., Suszczewicz, K.E., Borja, C.I., Cline, M.P., Hemmingsen, S.J., Qiji, S., Hobgood, H. M., Mizgerd, J.P., Sahoo, M.K., Zhang, H., Solis, D., Montine, T.J., Berry, G.J., Reiman, E.M., Röltgen, K., Boyd, S.D., Pinsky, B.A., Zehnder, J.L., Talbot, P., Desforges, M., DeTure, M., Dickson, D.W., Beach, T.G., 2022. SARS-CoV-2 Brain Regional Detection, Histopathology, Gene Expression, and Immunomodulatory Changes in Decedents with COVID-19. J Neuropathol Exp Neurol. 81 (9), 666–695.
Seubert, J., Freiherr, J., Djordjevic, J., Lundström, J.N., 2013. Statistical localization of human olfactory cortex. Neuroimage 66, 333–342. https://doi.org/10.1016/j.neuroimage.2012.10.030.
Shepherd, G.M., 2005. Perception without a thalamus how does olfaction do it? Neuron 46 (2), 166–168. https://doi.org/10.1016/j.neuron.2005.03.012.
Spudich, S., Nath, A., 2022. Nervous system consequences of COVID-19. Science 375 (6578), 267–269. https://doi.org/10.1126/science.abm2052.
Tabacof, L., Tosto-Mancuso, J., Wood, J., Cortes, M., Kontorovich, A., McCarthy, D., Rizk, D., Rozanski, G., Breyman, E., Nasr, L., Kellner, C., Herrera, J.E., Putrino, D., 2022. Post-acute COVID-19 Syndrome Negatively Impacts Physical Function, Cognitive Function, Health-Related Quality of Life, and Participation. Am J Phys Med Rehabil. 101 (1), 48–52.
Tobia, M.J., Yang, Q.X., Karunanayaka, P., 2016. Intrinsic intranasal chemosensory brain networks shown by resting-state functional MRI. Neuroreport 27 (7), 527–531. https://doi.org/10.1097/WNR.0000000000000579.
van den Heuvel, M.P., de Lange, S.C., Zalesky, A., Seguin, C., Yeo, B.T.T., Schmidt, R., 2017. Proportional thresholding in resting-state fMRI functional connectivity networks and consequences for patient-control connectome studies: Issues and recommendations. Neuroimage 152, 437–449. https://doi.org/10.1016/j.neuroimage.2017.02.005.
Voruz, P., Allali, G., Benzakour, L., Nuber-Champier, A., Thomasson, M., Jacot de Alcântara, I., Pierce, J., Lalive, P.H., Lövblad, K.-O., Braillard, O., Coen, M., Serratrice, J., Pugin, J., Ptak, R., Guessous, I., Landis, B.N., Assal, F., Péron, J.A., 2022. Long COVID neuropsychological deficits after severe, moderate, or mild infection. Clin Transl Neurosci. 6 (2), 9.
Voruz, P., Cionca, A., Jacot de Alcântara, I., et al., 2023. Brain functional connectivity alterations associated with neuropsychological performance 6–9 months following SARS-CoV-2 infection. Hum Brain Mapp. 44 (4), 1629–1646. https://doi.org/10.1002/hbm.26163.
Xydakis, M.S., Albers, M.W., Holbrook, E.H., Lyon, D.M., Shih, R.Y., Frasnelli, J.A., Pagenstecher, A., Kupke, A., Enquist, L.W., Perlman, S., 2021. Post-viral effects of COVID-19 in the olfactory system and their implications. Lancet Neurol. 20 (9), 753–761.
Yildirim, D., Kandemirli, S.G., Tekcan Sanli, D.E., Akinci, O., Altundag, A., 2022. A Comparative Olfactory MRI, DTI and fMRI Study of COVID-19 Related Anosmia and Post Viral Olfactory Dysfunction. Acad Radiol. 29 (1), 31–41. https://doi.org/10.1016/j.acra.2021.10.019.
Zalesky, A., Fornito, A., Bullmore, E.T., 2010. Network-based statistic: Identifying differences in brain networks. Neuroimage 53 (4), 1197–1207. https://doi.org/10.1016/j.neuroimage.2010.06.041.
Zhang, H., Chung, T.W.H., Wong, F.K.C., Hung, I.F.N., Mak, H.K.F., 2022. Changes in the Intranetwork and Internetwork Connectivity of the Default Mode Network and Olfactory Network in Patients with COVID-19 and Olfactory Dysfunction. Brain Sci. 12 (4), 511. https://doi.org/10.3390/brainsci12040511.